

SUPPORTING INFORMATION FOR MANUSCRIPT

NMR crystallography of α -Poly(L-lactide)

Tomasz Pawlak¹, Magdalena Jaworska¹ and Marek J. Potrzebowski¹.

1) Polish Academy of Sciences, Centre of Molecular and Macromolecular Studies, Sienkiewicza 112,
90-363 Lodz, Poland.

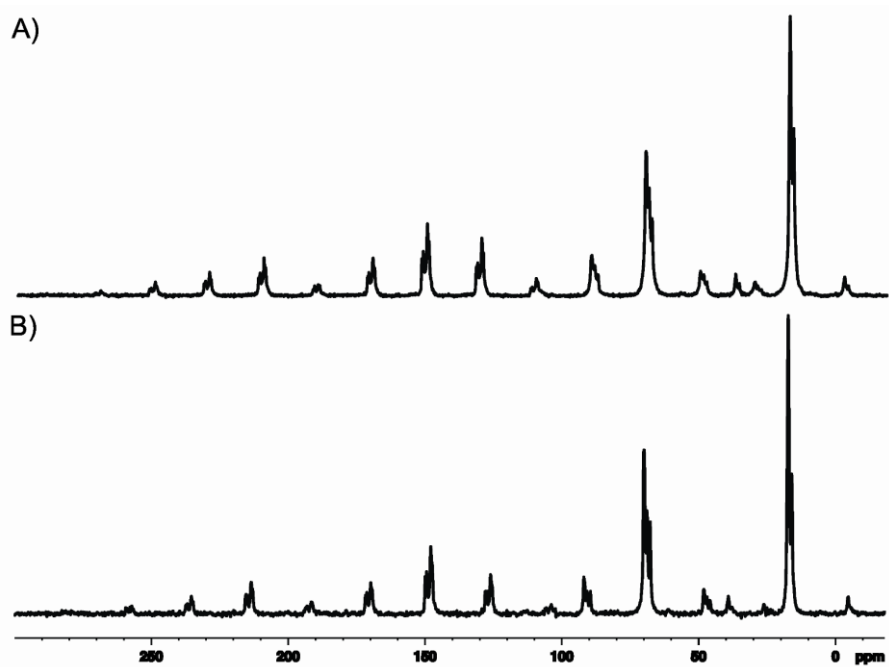


Figure S1. Experimental 1D ^{13}C CP MAS NMR spectra of α -PLLA-L (A) and α -PLLA-H (B) collected at a spinning rate of 2.2 kHz.

Experimental section

The ^{13}C - ^1H PISEMA MAS experiment was recorded with a proton 90° pulse length of $5\ \mu\text{s}$ at CP, a proton 90° pulse length of $2.5\ \mu\text{s}$ at SEMA, contact time of 1 ms, repetition delay of 3 s, time domain size of 1024 data points in F2 and 64 data points in F1, at a 13 kHz spinning rate.¹

A $5\text{-}\pi$ pulse 2D PASS scheme and 2.2 or 1.2 kHz sample spinning rates were used in the 2D experiments. The π -pulse length was $8\ \mu\text{s}$. Sixteen t_1 increments using the timings described by Levitt and co-workers were used in the 2D PASS experiments.² For each increment, 360 scans were accumulated. Because the pulse positions in the t_1 set return to their original positions after a full cycle and the t_1 -FID forms a full echo, the 16-point experimental t_1 data were replicated to 256 points. After the Fourier transformation in the direct dimension, the 2D spectrum was sheared to align all side bands with the center bands in the indirect dimension of the 2D spectrum. One-dimensional CSA spinning sideband patterns were obtained from t_1 slices taken at the isotropic chemical shifts in the t_2 dimension of the 2D spectrum. The magnitudes of the principal elements of the CSA tensor were obtained from the best-fit simulated spinning sideband pattern. Simulations of the spinning CSA sideband spectra were performed on a PC using the Topspin program.

Results and discussion

1. Precise assignment of the ^{13}C Chemical-Shift Parameters (CSTs) for α -PLLA. In our strategy, the crucial step is the accurate measurement of the chemical-shift tensor (CST) parameters. CST parameters can be obtained from analysis of the static line shape of ^{13}C nuclei. Static CST principal component measurements can be only used with simple molecules or simple labeling schemes because of spectral overlap and also suffer from sensitivity issues in natural abundance systems; 1D CP/MAS methods suffer from similar limitations. An alternative approach relies on the assignment the anisotropy and asymmetry of CSA by fitting the observed MAS sideband intensities.³ For accurate results to be obtained, it is necessary that numerous spinning sidebands be present in the spectrum: approximately 5 significant spinning sidebands are needed to determine the anisotropy (for asymmetry parameters in the range $0.1 < \eta < 1$), whereas 6–10 sidebands are required to determine the asymmetry ($0.3 < \eta < 1$). By employing the Herzfeld–Berger analysis protocol, the anisotropy, asymmetry and chemical shift tensor (CST) parameters can be obtained.⁴

Figure S 2 shows the ^{13}C CP MAS NMR spectra of α -PLLA recorded at ambient temperature with spinning rates of 8 kHz, 2.2 kHz and 1.2 kHz. The high crystallinity of sample is apparent from

inspection of the spectrum measured with a high spinning speed (Figure S2 A). The splitting of signals is observed in the carbonyl, methine and methyl regions.

Unfortunately, the spectrum measured with a spinning speed of 8 kHz does not contain spinning sidebands. As evident from the figure, the spectra recorded with spinning speeds of 2.2 kHz (Figure S2 B) and 1.2 kHz (Figure S2 C) represent patterns with a sufficient number of spinning sidebands for fine analysis of CST for both the carbonyl groups and the aliphatic residues. However, at a low MAS frequency, the sideband manifold makes the assignment of the CST parameters ambiguous. This ambiguity establishes the need for 2D NMR techniques.

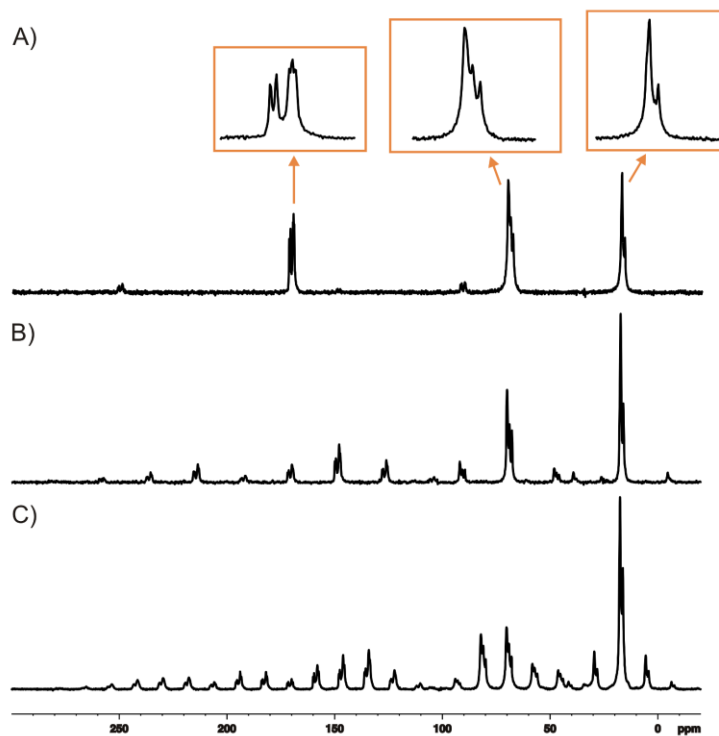


Figure S2. ^{13}C CP MAS NMR spectra of α -PLLA recorded with a spinning rate of A) 8 kHz, B) 2.2 kHz and C) 1.2 kHz. Insets in Figure A show expanded signals with splittings typical of a highly crystalline sample.

Several approaches exist that allow the separation of the isotropic and anisotropic portions of the spectra for a heavy overlapped system.^{5,6,7,8} In this work, we employed the 2D PASS sequence for the analysis of the ^{13}C spectra.²

This technique offers good sensitivity compared to other methods and does not require hardware modifications or a special probe head. The 2D PASS spectra of PLLA recorded with spinning rates of 2.2 and 1.2 kHz are attached as Supplementary Information. The ^{13}C δ_{ii} values were established using the procedure reported in our previous papers.⁹ To ensure that CST parameters were elucidated with high accuracy, we introduced a double-checking procedure by fitting 1D spectra under slow rotation with ^{13}C δ_{ii} elements taken from the 2D PASS measurements. Figures S3A and S3 B display experimental and calculated spectra of PLLA recorded with a spinning rate of 1.2 kHz. Figure S3 C shows a set of calculated subspectra that represent each assigned NMR position. The sum of the subspectra correlate well with the spinning sideband pattern. The ^{13}C δ_{ii} parameters used for the simulation of the spectra under slow rotation are collected in Table 1 (see main text).

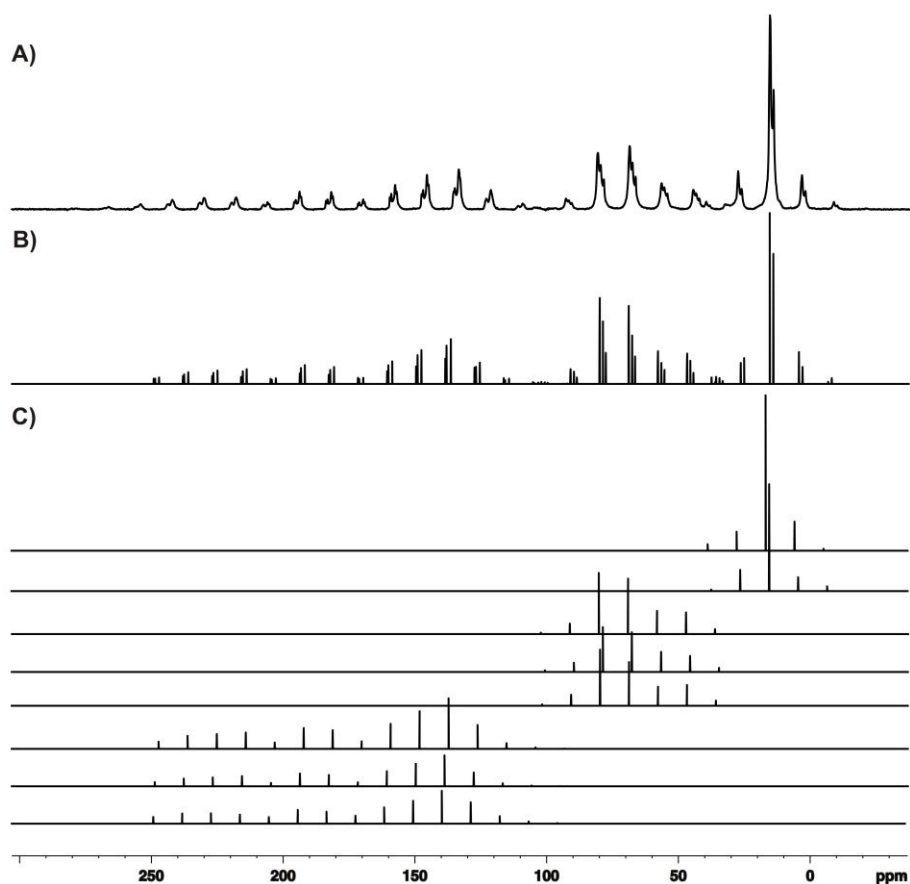


Figure S3. Experimental and calculated 1D spectra of α -PLLA. Figure A shows the experimental spectrum recorded with a spinning rate of 1.2 kHz. Figure B shows a stick model spectrum calculated with ^{13}C δ_{ii} parameters taken from 2D PASS measurements. Figure C displays appropriate subspectra for each assigned carbon position.

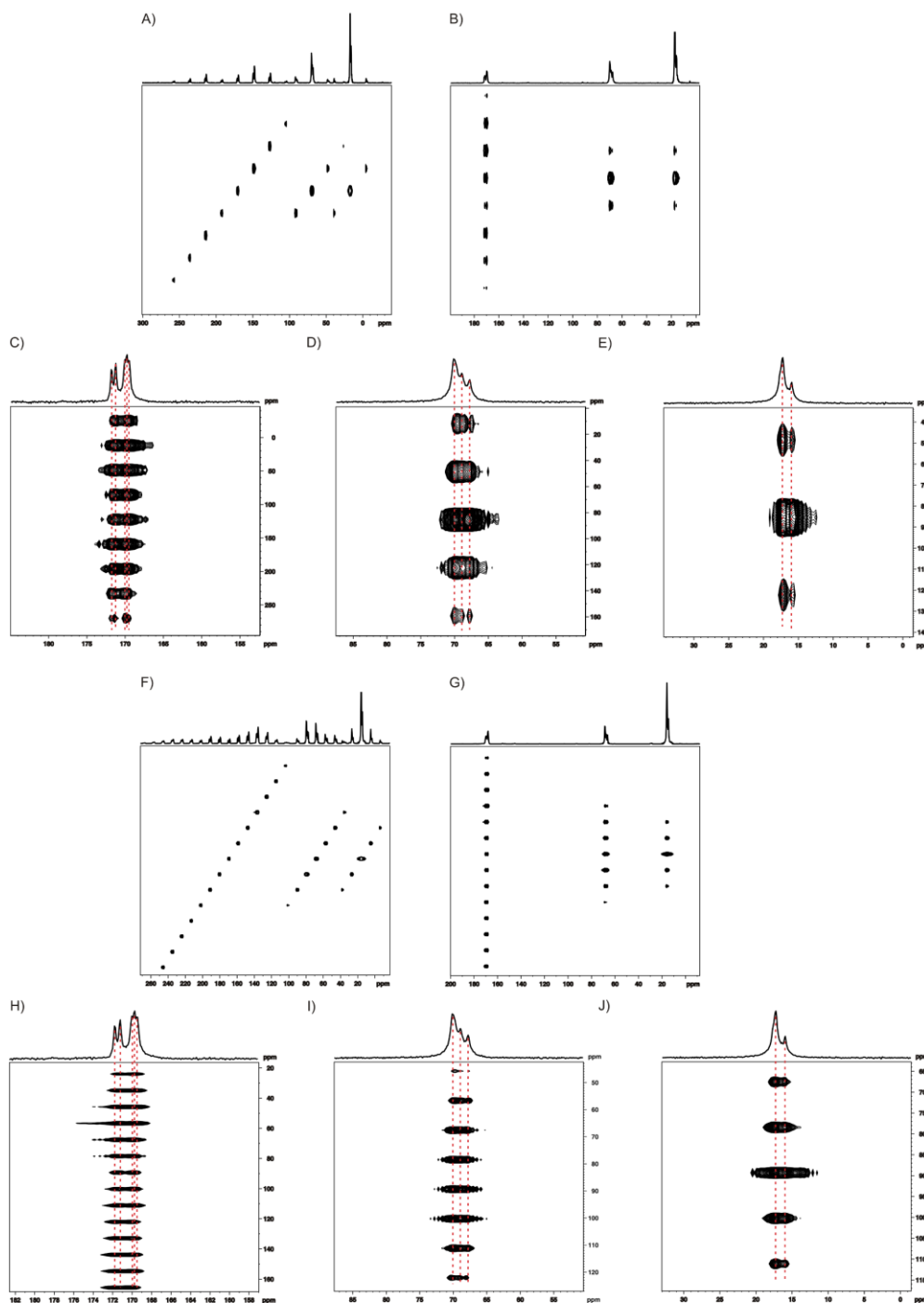
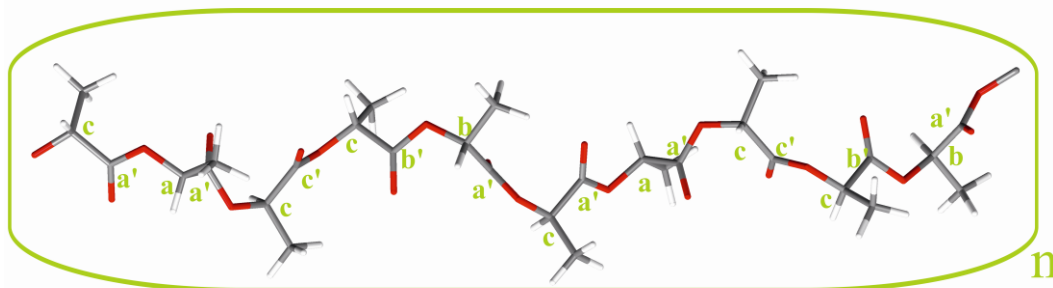


Figure S4. 2D PASS spectra for α -Poly(L-lactide) recorded with a spinning rate of 2.2 kHz: (A) and after data shearing (B), (C-E) appropriate magnifications of C=O, CH and CH₃ groups and 1.1 kHz: (F) and after data shearing (G); (H-J) appropriate magnifications of C=O, CH and CH₃ groups.



Scheme S1 10^3 -Helix α -PLLA and its numbering system according to experimental results (Table 1). Carbonyl groups are labeled with primes (n')

2. Analysis of the molecular dynamics for α -PLLA. Dynamic processes are well known strongly influence CST tensor values. The correlations between experimental and computed NMR parameters for solid systems with small and large amplitude motions have been recently reported by several research groups.¹⁰ Clearly, knowledge about the possible molecular motions for the sample under investigation is a prerequisite to the development of a viable NMR crystallography strategy.

The problems associated with the molecular dynamics of PLLA were recently discussed by Pan et al.^{32b}, who employed temperature-variable FTIR and solid-state ^{13}C NMR to reveal the differences between the polymorphs of PLLA. They used the ^{13}C T_1 relaxation time as a diagnostic NMR parameter to discriminate between the different forms. Unfortunately, spin–lattice relaxation time is not particularly sensitive to local molecular motion; it rather provides information about global dynamics. To gain precise information about the molecular motion of each carbon bonded to hydrogen, we have employed a technique based on dipolar recoupling experiments, which are well suited for the simultaneous measurement of motional averaging at multiple sites.^{11,12,13} In the two-dimensional (2D) experiments, the separated local field sequences can reintroduce dipolar anisotropic interactions and correlate them to the isotropic chemical shifts.¹⁴ The Lee–Goldburg cross-polarization (LGCP)^{15,16,17} and polarization inversion spin exchange at the magic angle (PISEMA)¹⁸ pulse sequences were recently used to correlate the motional average anisotropic dipolar interactions with high-resolution chemical-shift dimensions during MAS in the 2D approach. For analysis of the effect of molecular motion on the line shape of the dipolar spectra, we have employed a modified sequence of PISEMA MAS, as reported by Dvinskikh et al.¹ Figure S4 A displays the 2D PISEMA MAS spectrum for PLLA recorded with a spinning rate of 13 kHz at ambient temperature. Figure S4 B shows expanded regions of CH and CH_3 carbons. The ^1H effective

field strength, ω_{Heff}^1 , was held constant, whereas the ^{13}C spin-lock field strength was matched using $\omega_{\text{Heff}}^1 \pm \omega_{\text{C}}^{13} = n\omega_r$ ($n = 1, -1$). The SEMA contact time was increased asynchronously with rotation to yield the heteronuclear dipolar dimension of the 2D experiment. The ^{13}C spin isotropic chemical shift was detected in the second dimension of the experiment. Figure S4 C shows the F1 slices for the CH and CH_3 residues with labeled splitting between the singularities of the doublets. These doublets reflect the dipolar coupling between the proton and carbon.

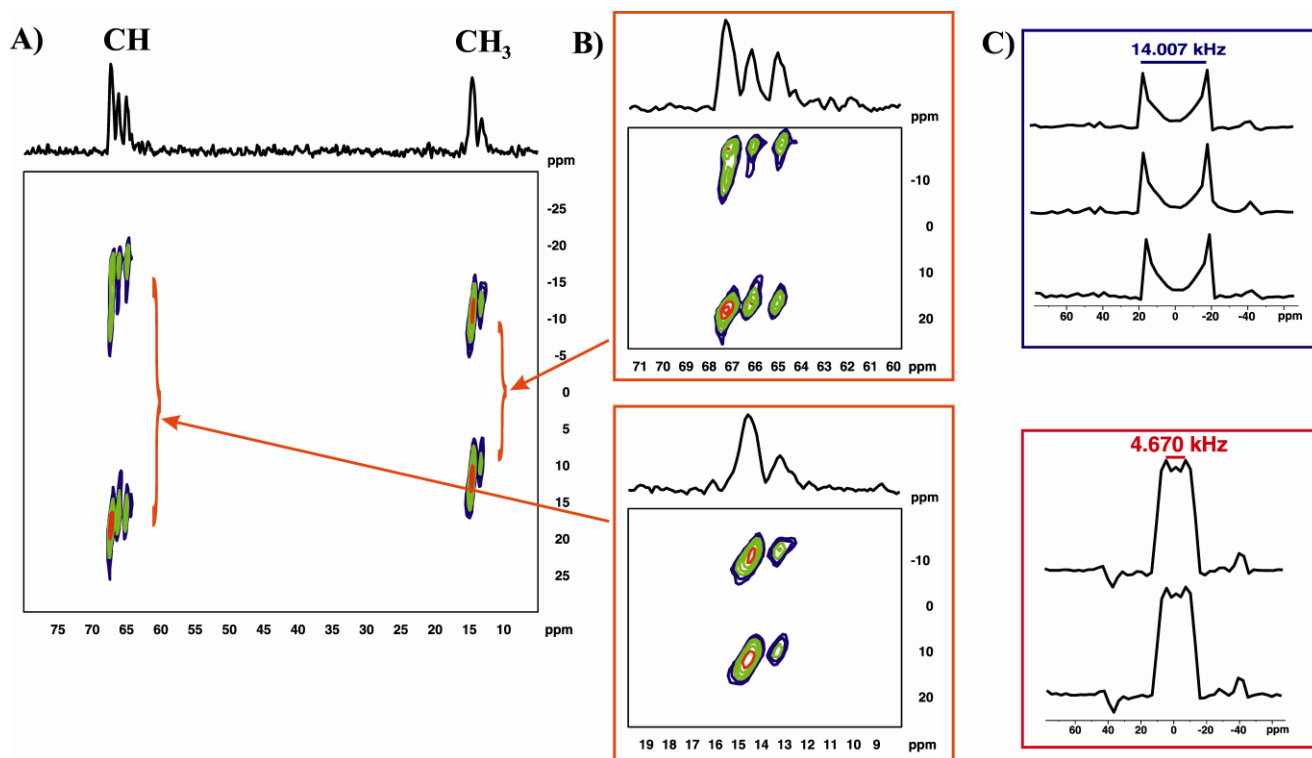


Figure S5. A) 2D correlation PISEMA MAS of ^{13}C chemical shifts and ^1H - ^{13}C dipolar couplings for α -PLLA (at a spinning rate of 13 kHz); B) the magnified regions for -CH and - CH_3 groups; C) the experimental dipolar spectra for -CH and - CH_3 groups, including values of dipolar couplings.

For ^{13}C - ^1H , the r_{ij} distance is equal to 1.07 Å, the dipolar coupling constant D for the rigid-limit is 24.0 kHz according to the following equation.

$$D = -\frac{\mu_0 \hbar^2 \gamma_i \gamma_j}{4\pi r_{ij}^3}$$

The experimental values of the splitting shown in Figure S4 C are smaller than the calculated coupling values because D is reduced by a scaling factor (sf). For the PISEMA MAS, the exact Hartmann-Hahn matching condition yields a maximum scaling factor of 0.584 ($\cos 54.7^\circ$). For the rigid system, the expected value of D is ca. 14.0 kHz (24 kHz \cdot 0.584). Fast molecular motion can reduce the principal component of the dipolar tensor by a factor (S), which is known as the order parameter. The value of S ranges from 0.5 to 1, where the latter value represents a rigid system.

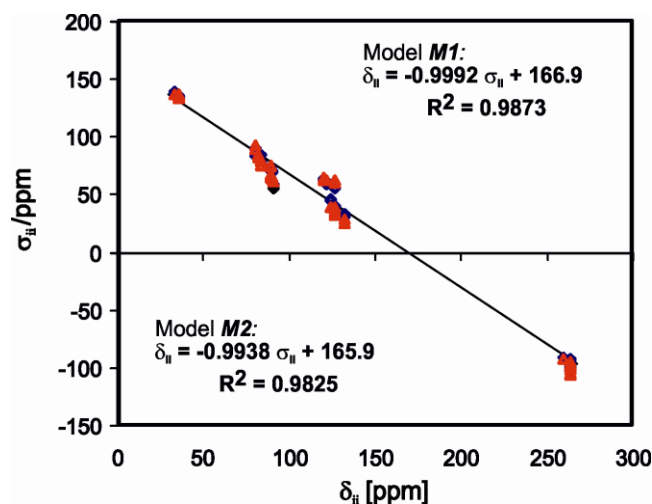


Figure S6. Correlation of experimental chemical shift tensor values (δ_{ii}) with calculated nuclear shielding parameters (σ_{ii}) of a-PLLA using model *M1* (blue) and *M2* (red).

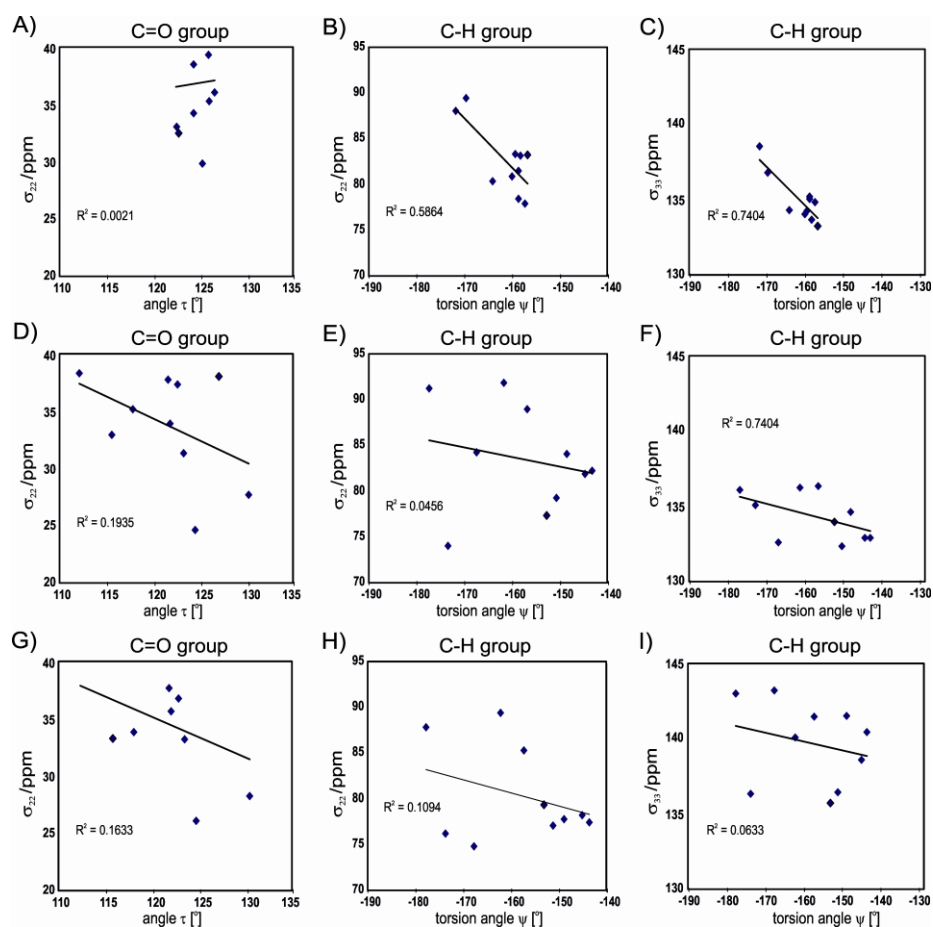


Figure S7. The correlation between σ_{22} and the valence angle τ for the C=O groups (A, D, G). As well as the correlations between the torsion angle ψ and σ_{22} (B, E, H) and σ_{33} (C, F, I) for the CH groups. The σ_{ii} parameters were calculated using model *M1* (A – C), *M2* (D – F) and *M3* (G – I).

Table S1. NMR chemical shift tensors [in ppm] for model *MI*.

Position	σ_{iso}	σ_{11}	σ_{22}	σ_{33}
1	95.2	69.5	83.1	133.1
2	98.5	69.6	89.3	136.5
3	95.2	71.3	80.3	134.1
4	95.1	73.0	77.8	134.6
5	91.0	58.5	80.8	133.9
6	95.3	69.3	83.1	133.5
7	98.3	68.7	87.9	138.2
8	96.1	71.1	83.2	134.0
9	95.6	70.3	81.4	135.0
10	89.1	54.1	78.3	134.8
1'	-1.9	-99.2	32.6	60.8
2'	3.6	-95.6	44.2	62.1
3'	-3.1	-101.1	33.2	58.6
4'	-0.1	-92.4	29.9	62.2
5'	-3.1	-103.2	39.5	54.5
6'	-0.8	-100.5	38.6	59.6
7'	4.4	-93.1	45.8	60.4
8'	-0.2	-97.2	36.2	60.5
9'	1.1	-92.3	34.3	61.4
10'	-4.2	-103.2	35.4	55.2

Table S2. NMR chemical shift tensors [in ppm] for model *M2*.

Position	σ_{iso}	σ_{11}	σ_{22}	σ_{33}
1	95.1	73.9	77.4	134.0
2	97.5	64.3	91.8	136.3
3	94.1	73.2	74.0	135.1
4	94.5	66.7	84.2	132.6
5	96.0	62.7	88.9	136.4
6	93.7	62.3	84.0	134.7
7	97.3	64.5	91.3	136.1
8	91.9	60.9	81.9	132.9
9	92.9	63.4	82.2	132.9
10	89.8	57.6	79.3	132.4
1'	2.3	-93.4	38.2	62.2
2'	0.4	-98	35.4	63.9
3'	-0.3	-93.6	31.4	61.3
4'	-0.9	-95.2	33	59.4
5'	0.0	-99.7	37.9	61.9
6'	-1.2	-99.2	34	61.5
7'	-0.7	-102.5	38.5	61.9
8'	-6.8	-106.6	24.6	61.6
9'	-5.5	-106.2	27.8	62
10'	0.3	-99	37.5	62.3

Table S3. NMR chemical shift tensors [in ppm] for model *M3*.

Position	σ_{iso}	σ_{11}	σ_{22}	σ_{33}
1	96.6	74.5	79.6	135.7
2	98.8	66.5	89.7	140.1
3	95.6	74.0	76.4	136.3
4	95.8	69.3	75.0	143.2
5	96.9	63.7	85.5	141.5
6	92.4	57.8	77.9	141.5
7	99.6	67.7	88.1	143.0
8	93.0	62.0	78.4	138.6
9	93.4	62.1	77.7	140.4
10	91.1	59.6	77.3	136.4
1'	3.4	-92.9	40.4	62.5
2'	-0.4	-98.1	33.9	63.2
3'	1	-92.6	33.2	62.2
4'	-1.1	-96.7	33.3	60.1
5'	0.1	-99	37.8	61.6
6'	0.4	-97.6	35.7	63.2
7'	0	-102.4	40.4	61.9
8'	-5.7	-104.7	26	61.7
9'	-4.1	-105.2	28.2	64.6
10'	0.4	-98.1	36.9	62.5

Table S4. NMR chemical shift tensors [in ppm] for model *M4* using PBE functional.

Position	σ_{iso}	σ_{11}	σ_{22}	σ_{33}
1	94.9	73.9	77.1	133.8
2	94.4	66.6	84.1	132.4
3	97.2	64.4	90.9	136.2
4	97.4	63.9	91.9	136.3
5	95.9	62.5	88.8	136.4
6	91.9	60.9	81.8	132.9
7	94.0	73.0	73.8	135.1
8	90.9	56.5	79.1	137.2
9	93.0	61.0	80.5	137.4
10	89.7	57.6	79.0	132.6
1'	2.2	-93.6	38.1	62.1
2'	-1.0	-95.5	32.5	59.9
3'	-0.8	-102.7	38.4	61.8
4'	0.3	-97.9	35.1	63.6
5'	-0.1	-99.2	37.6	61.4
6'	-7.3	-106.7	23.6	61.3
7'	-0.4	-93.6	31.3	61.2
8'	-0.4	-98.6	34.4	62.9
9'	-4.6	-106	27.9	64.4
10'	0.2	-99.2	37.5	62.3

Table S5. NMR chemical shift tensors [in ppm] for model *M4* using PW91 functional.

Position	σ_{iso}	σ_{11}	σ_{22}	σ_{33}
1	96.3	56.6	74.5	83.3
2	96.1	58.2	73.3	83.6
3	99.2	63.3	72.7	88.6
4	99.1	63.2	72.8	88.4
5	97.6	64.4	70.4	87.8
6	97.2	60.7	73.1	84.8
7	97.4	60.6	73.4	84.7
8	96.5	58.1	73.9	83.5
9	96.1	58.8	72.8	83.8
10	97.3	64.1	70.3	87.1
1'	-5.7	161.8	-108.1	37.3
2'	-7.8	160.1	-105.1	26.8
3'	-6.4	161.4	-108.2	35.9
4'	-6.2	161.0	-107.8	35.9
5'	-6.7	161.7	-107.4	33.1
6'	-8.6	163.2	-109.0	29.1
7'	-8.5	163.0	-108.7	29.1
8'	-5.5	161.9	-107.7	36.9
9'	-8.0	159.3	-105.1	27.0
10'	-6.7	161.9	-107.6	33.2

Table S4. NMR chemical shift tensors [in ppm] for model *M4* using RPBE functional.

Position	σ_{iso}	σ_{11}	σ_{22}	σ_{33}
1	97.0	55.6	75.9	83.5
2	96.2	58.5	73.4	83.4
3	99.6	61.7	74.2	88.7
4	99.6	61.5	74.4	88.5
5	98.2	64.4	70.7	88.8
6	97.6	60.4	73.6	85.2
7	97.6	60.3	73.6	85.2
8	96.9	56.4	75.4	83.5
9	96.3	59.3	73.0	83.5
10	98.2	64.5	70.7	88.5
1'	-3.2	160.7	-105.5	40.9
2'	-5.5	158.3	-102.9	31.1
3'	-4.0	159.5	-105.6	39.7
4'	-4.0	159.1	-105.3	39.6
5'	-4.4	160.4	-105.3	37.0
6'	-6.4	161.3	-106.5	32.7
7'	-6.3	161.5	-106.6	32.8
8'	-3.1	160.6	-105.4	40.9
9'	-5.5	158.0	-102.7	31.0
10'	-4.4	161.0	-105.3	36.5

REFERENCES

- (1) (a) S. V. Dvinskikh, H. Zimmermann, A. Maliniak, D. Sandström, *J. Magn. Reson.*, 2003, **164**, 165; (b) K. Yamamoto, D. K. Lee, A. Ramamoorthy, *Chem. Phys. Lett.*, 2005, **407**, 289.
- (2) O. N. Antzutkin, S. C. Shekar, M. H. Levitt, *J. Magn. Reson., Ser. A*, 1995, **115**, 7.
- (3) (a) P. Hodgkinson, L. Emsley, *J. Chem. Phys.*, 1997, **107**, 4808; (b) A. C. Olivieri, *Magn. Reson. A*, 1996, **123**.
- (4) J. Herzfeld, A. E. Berger, *J. Chem. Phys.*, 1980, **73**, 6021.
- (5) J. Hu, W. Wang, F. Liu, M. S. Solum, D. W. Alderman, R. J. Pugmire, *J. Magn. Reson. Ser. A*, 1995, **113**, 210.
- (6) D. W. Alderman, G. McGeorge, J. Z. Hu, R. J. Pugmire, D. M. Grant, *Mol. Phys.* 1998, **95**, 1113.
- (7) L. Frydman, G. C. Chingas, Y. K. Lee, P. J. Grandinetti, M. A. Eastman, G. A. Barral, A. Pines, *J. Chem. Phys.*, 1992, **97**, 4800.
- (8) A. C. Kolbert, R. G. Griffin, *Chem. Phys. Lett.*, 1990, **166**, 87.
- (9) (a) M. Jaworska, P. B. Hrynczyszyn, M. Wełniak, A. Wojtczak, K. Nowicka, G. Krasiński, H. Kassassir, W. Ciesielski, M. J. Potrzebowski, *J. Phys. Chem. A* 2010, **114**, 12522.
- (10) (a) T. Pawlak, K. Trzeciak-Karlikowska, J. Czernek, W. Ciesielski, M. J. Potrzebowski, *J. Phys. Chem. B*, 2012, **116**, 1974; (b) E. Carignani, S. Borsacchi, A. Marini, B. Mennucci, M. Geppi, *J. Phys. Chem. C*, 2011, **115**, 25023; (c) J. N. Dumez, C J. Pickard, *J. Chem. Phys.* 2009, **130**, 104701; (d) I. De Gortari, G. Portella, X. Salvatella, V. S. Bajaj, P. C. van der Wel, J. R. Yates, M. D. Segall, C. J. Pickard, M. C. Payne, M. Vendruscolo, *J. Am. Chem. Soc.* 2010, **132**, 5993.
- (11) V. Ladizhansky, *Solid State Nucl. Mag.* 2009, **36**, 119.

- (12) Wylie, B. J.; Rienstra, C. M. *J. Chem. Phys.* 2008, **128**, 052207.
- (13) G. P. Drobny, J. R. Long, T. Karlsson, W. Shaw, J. Popham, N. Oyler, P. Bower, J. Stringer, D. Gregory, M. A. Mehta, P. S. Stayton, *Annu. Rev. Phys. Chem.* 2003, **54**, 531.
- (14) K. Schmidt-Rohr, H. W. Spiess, *Multidimensional Solid-State NMR And Polymers*; Academic Press: London, 1994.
- (15) M. F. Cobo, K. Malinakova, D. Reichert, K. Saalwachter, E. R. Deazevedo, *Phys. Chem. Chem. Phys.*, 2009, **11**, 7036.
- (16) V. Ladizhansky, S. Vega, *J. Chem. Phys.*, 2000, **112**, 7158.
- (17) M. Hong, X. Yao, K. Jakes, D. Huster, *J. Phys. Chem. B*, 2002, **106**, 7355.
- (18) A. Ramamoorthy, Y. Wei, D. K. Lee, *Annu. Rep. NMR Spectros.*, 2004, **52**, 1.